

Electrochemical Reduction Behavior of Alizarin Red S at HMDE in Aqueous Solutions

Refat Abdel-Hamid,* Mostafa K. Rabia, and Hussein M. El-Sagher

Department of Chemistry, Faculty of Science, South Valley University, Sohag, Egypt

(Received March 12, 1997)

At hanging mercury-drop electrode (HMDE) Alizarin Red S (ARS) is electrochemically reduced in aqueous buffer solutions, giving rise to a prominent wave and a pre-wave. The prominent wave is diffusion-controlled and involves two electrons and two protons. The pre-wave is attributed to a strong reversible adsorption of the reduction product at the electrode. The reduction mechanism was proposed and discussed on the basis of the cyclic voltammetric and double potential-step chrono-amperometric & coulometric results. It was concluded that the reduction pathway is an ECEC mechanism in which the chemical reactions (C) are a dimerization of the formed radical anion and protonation of the dianion dimer, respectively. The rate-determining step is the protonation reaction. The adsorption process obeys a Langmuir isotherm with maximum surface excess of 1.4×10^{-10} mol cm⁻² at a bulk concentration $\geq 4.6 \times 10^{-5}$ mol dm⁻³, corresponding to 1.18 nm²/molecule. This indicates that ARS is horizontally oriented and resists reorientation upon increasing its bulk concentration.

The electrochemistry of anthraquinones has received much attention because of their relevance to some important electrochemical processes.¹ For example anthraquinone disulphonate was used to build photocathode–dark anode and photoanode–dark cathode rechargeable solar cells.² Anthraquinone-2-sulphonate acts as a mediator for the electrode reactions at lipid-coated electrodes by transferring ions or electrons across its adsorbed monolayer.³ They display an interesting electrochemical behavior due to their quinonoid structure.⁴ The electrochemical behavior depends as much on the nature of the derivative as on the medium. The most important feature of quinones is the reversible reduction via a one-electron-transfer to the semiquinone species, which has a radical structure. These are apparently involved in many biological systems, such as photosystem-II of green plant photosynthesis,^{5,6} as well as many other biological electron-transfer chains.^{7,8} A better understanding of the redox chemistry of these compounds will enhance our knowledge of the charge-transfer mechanism involved in biological systems.

Alizarin Red S was studied earlier polarographically at a dropping mercury electrode^{9–13} and voltammetrically at a rotated pyrolytic graphite electrode.¹⁴ It was concluded that the reagent forms semiquinone on the reduction by taking up a single electron; the uptake of a further electron results in the formation of hydroquinone. Whether under the given experimental circumstances a single two-electron voltammetric wave or two single-electron waves is observed depends on the stability of the semiquinone. Each of the reduction products involve a different degree of protonation. No detailed investigation on the electrochemical reduction mechanism and adsorption behavior of Alizarin Red S was found. Thus, it seems of interest to investigate the reduction mechanism and adsorption behavior in detail to obtain better insight into

its electrochemical behavior. This can be done by carrying out a more thorough electrochemical investigation than those reported earlier as well as parametrization of the electrode reaction. A reduction mechanism in bulk and in adsorbed state is proposed and a quantitative explanation for the behavior is provided. The study was performed in aqueous buffer solutions of different pH's at a hanging mercury-drop electrode utilizing cyclic voltammetry and double potential step chronoamperometry & chronocoulometry.

Experimental

Reagents and Solutions: Alizarin Red S of analytical-grade purity was used. A stock solution of fresh 5.0 mM in triple-distilled water was prepared, kept in an inert nitrogen atmosphere and diluted as required. Britton–Robinson universal buffer solutions were prepared from analytical-grade chemicals.

Instrumentation: The cell and the instruments used for cyclic voltammetry, double potential step chronoamperometry and chronocoulometry were described elsewhere.¹⁵ For all experiments a Ag/Ag⁺ electrode was used as a reference electrode. The hanging mercury-drop electrode (HMDE) in hanging drop mode was used throughout. The electrode area was 3.41×10^{-5} cm². All measurements were obtained at 298 K. Solutions were deaerated by purging with pure nitrogen before measurements, and a blanket of nitrogen was maintained above the working solution.

Results and Discussion

The electrochemical behavior of 6.0×10^{-4} mol dm⁻³ Alizarin Red S, sodium 1,2-dihydroxy anthraquinone-3-sulphonate (ARS) was investigated in Britton–Robinson universal buffer solutions over a pH range of 1.68–9.85 using cyclic voltammetry at a hanging mercury-drop electrode (HMDE). Generally, a cyclic voltammogram of ARS exhibits a prominent wave and a pre-wave on the negative scan

throughout the whole pH range, c.f. Fig. 1. On a reverse scan, two anodic voltammetric waves are observed at more positive potentials.

At pH 1.68, Alizarin Red S gives a quasireversible prominent voltammetric reduction wave in the potential range of 0.0 to -0.60 volt versus Ag/Ag⁺ at a scan rate of 50 mV s⁻¹. Cyclic voltammograms of 6.0 × 10⁻⁴ mol dm⁻³ Alizarin Red S at different scan rates are shown in Fig. 1. The peak separation ($\Delta E_p = E_{pc} - E_{pa}$ cathodic to anodic) is 77 mV at 50 mV s⁻¹, and increases upon increasing the scan rate. Its observed width ($E_p - E_{p/2}$) is 44 ± 2 mV, which is less than the expected theoretical value of a reversible one electron-transfer process, and is larger than that for the reversible two-electron-transfer one (56.5/n mV at 298 K).¹⁶⁾ The peak current ratio (i_{pa}/i_{pc}) computed from Eq. 1 increases upon increasing the scan rate. In Eq. 1, $i_{pa}(0)$ is the

$$\frac{i_{pa}}{i_{pc}} = \frac{i_{pa}(0)}{i_{pc}} + \frac{0.485 \times i_{\lambda}(0)}{i_{pc}} + 0.086 \quad (1)$$

uncorrected anodic peak current and $i_{\lambda}(0)$ is the uncorrected current at the switching potential (E_{λ}), both measured with respect to the zero current base line.¹⁷⁾ Moreover, the current function ($i_{pc}/v^{1/2}$) decreases with increasing the scan rate. It is found that the peak current potential of the diffusion wave varies with the reagent concentration. Furthermore, the log-log relation, peak current (i_{pc}) as a function of the scan rate (v) is linear with a slope of 0.49, indicating that the reduction process is due to the diffusing of ARS from the bulk to the electrode.^{16,18,19)} On the reverse scan, an anodic wave appears at more positive potentials. Consequently, these findings point to the initial hypothesis that the diffusion wave can be attributed to the electrochemical reduction of Alizarin Red S at lower pHs, 1.68, following an ECE mechanism in which E represents a reversible electron-transfer in which $E^{\circ}_1 = E^{\circ}_2$ ²⁰⁾ and C represents a reversible second-order dimerization reaction. Thus, it is possible to ascribe the oxidation wave to the oxidation of the product at the diffusion wave, i.e., the dimer resulting from the coupling of the formed free radicals. Upon increasing the scan rate from 50 to 1000 mV s⁻¹, a pre-peak tends to appear at 200 mV s⁻¹, and increases upon increasing the scan rate. The pre-peak is attributed to the adsorption of the reduction product, since the log-log relation has a slope of 1.01 at a bulk concentration of 5.0 × 10⁻⁶ mol dm⁻³.^{16,18,19)}

With increasing the pH of the solution, the diffusion wave and the adsorption pre-peak are shifted to more negative potentials. Thus, the reduction process over the entire pH range involves protons. Upon plotting the peak-current potential (E_p) as a function of the pH, two straight segments for the prominent diffusion wave and a straight line for the pre-peak are obtained. The two segments of the prominent wave intersect at a pH value of 5.2, which corresponds to the pK value of the subject compound. It is worth pointing out that this experimentally obtained value agrees well with that reported earlier for the 2-hydroxy group of Alizarin Red S.¹⁴⁾ The obtained linear least-squares relations can be represented as follows:

For diffusion wave:

$$E_p = -0.128 \pm 0.002 - 0.078 \pm 0.003 \text{ pH} \quad r = 0.992 \quad (2)$$

$$E_p = -0.250 \pm 0.002 - 0.052 \pm 0.001 \text{ pH} \quad r = 0.998 \quad (3)$$

and for adsorption pre-wave:

$$E_p = -0.065 \pm 0.002 - 0.076 \pm 0.002 \text{ pH} \quad r = 0.990 \quad (4)$$

The decrease in the slope of the E_p -pH relation for the prominent diffusion wave at pH's above 5.2 is probably due to the dissociation of the 2-hydroxy group. The number of protons involved in the reduction processes is estimated from the slopes ($dE_p/d\text{pH}$), since the expected value for these slopes is a simple multiple of the Nernstian pre-logarithmic constant of 60 mV/pH. For the main cv wave, it is found that two protons are involved, indicating that each electron transferred is matched by one proton, since a complete reduction of Alizarin Red S requires the uptake of two electrons.⁹⁻¹⁴⁾ It is worth noting that the slope of the adsorption pre-wave is higher than that expected based on the Nernstian pre-logarithm constant. Thus, the shift in its peak potentials is not only due to the proton dependence of the redox reaction involving adsorbed species, but also reflects a change in the adsorption strength of the reduced form relative to the oxidized form with the pH. The relatively faster peak potential shift towards the negative direction for the adsorbed redox couple suggests that the relative adsorption strength of the reduced form decreases with increasing pH of the solution.

In solutions of pH 6.75, 1.4 × 10⁻⁴ mol dm⁻³ Alizarin Red S exhibits a prominent quasireversible reduction peak and a pre-peak on the forward scan at a scan rate of 500 mV s⁻¹. On the reversal scan, an oxidation wave is observed c.f. Fig. 1. Upon decreasing the scan rate, the prominent peak shifts to less negative potentials, while the pre-peak does not, and the peak current decreases for both. The dependence of the peak current of the cathodic waves on the scan rate is tested by applying the log-log relation. This gives a linear dependence with slopes of 0.57 ± 0.02 for the main wave and 0.67 ± 0.01 for the pre-peak with correlation coefficients of 0.999, and 0.998, respectively. Furthermore, the peak current of the main wave linearly correlates with the concentration of the reagent (correlation coefficient = 0.999), while the pre-peak shows a Langmuir isotherm at lower concentrations, < 8.2 × 10⁻⁵ mol dm⁻³. Upon increasing the concentration, the pre-wave coalesces with the main wave. These findings indicate that the main wave is diffusion-controlled in nature and that the pre-wave is due to moderate adsorption of the reduction product of ARS.

The observed width of the cathodic wave ($E_p - E_{p/2}$) is 36 mV, slightly greater than the expected theoretical value of 28.2 mV for two-electron process at 298 K.²⁰⁾ The peak separation (ΔE_p) has a value of 58 mV. The peak current ratio (i_{pa}/i_{pc}) has a value of approximately 0.5. Furthermore, a slight increase in the current function ($i_p/v^{1/2}$) with the scan rate is observed. From the foregoing results, the electrochemical reduction of Alizarin Red S at pH 6.75 follows, along a prominent wave, ECE kinetics, as the initial

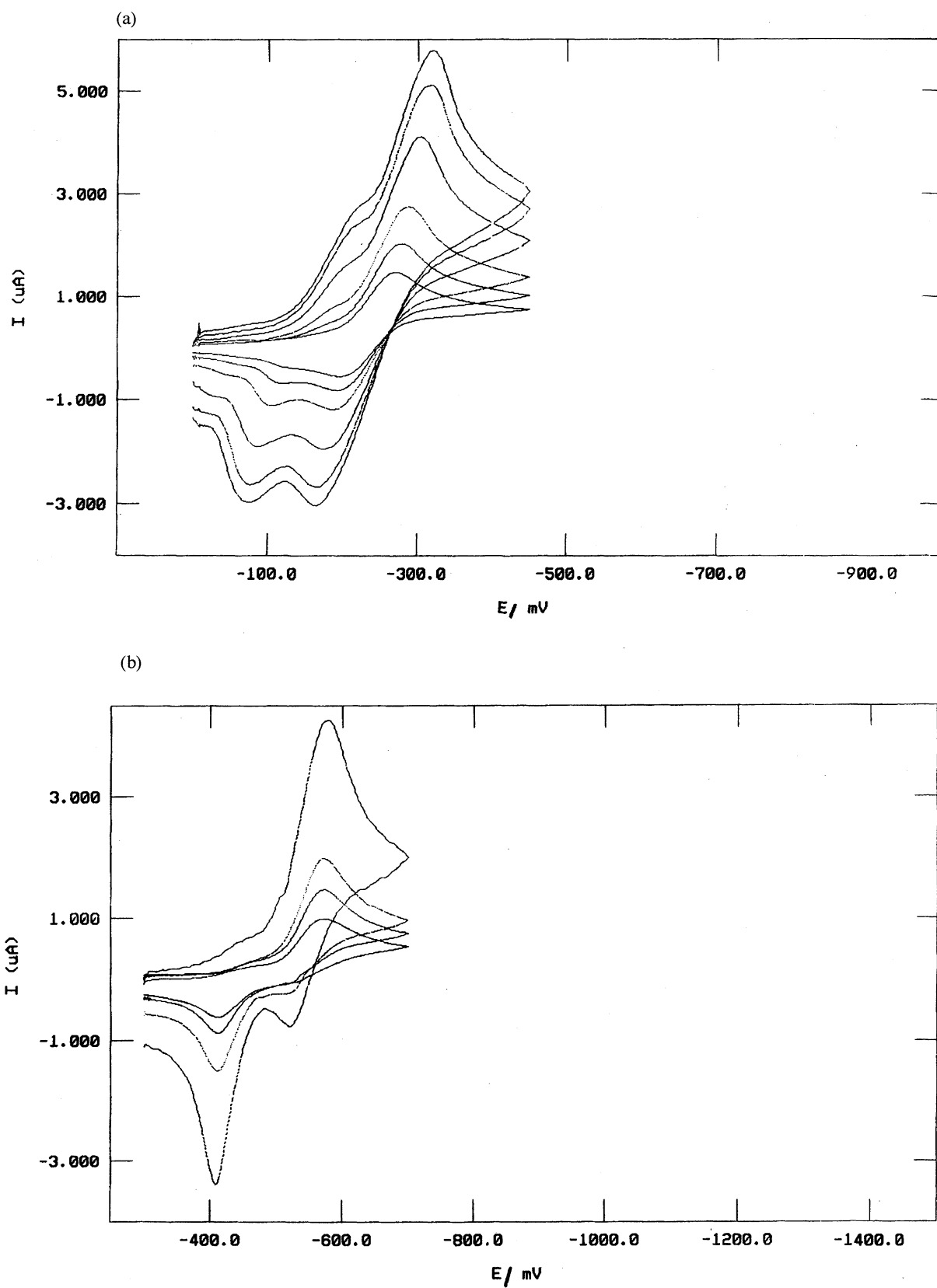


Fig. 1. Cyclic voltammograms of $6.0 \times 10^{-4} \text{ mol dm}^{-3}$ Alizarin Red S at scan rates of, (a) 50, 100, 200, 500, 800, and 1000 mV s^{-1} at pH=1.68. (b) 50, 100, 200, and 800 mV s^{-1} at pH=6.75.

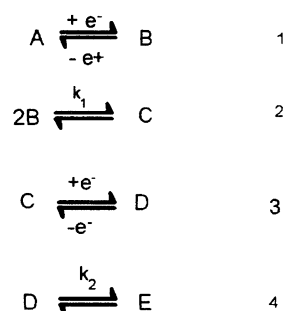
suggestion, in which the electron transfer processes (E) are reversible and the chemical reaction (C) is irreversible second-order dimerization. The appearance of an anodic wave, which is due to oxidation of the dimer product, supports the suggestion of dimerization.

Double potential step chronoamperometry and chronocoulometry are superior to cyclic voltammetry for studying the electrode reaction mechanisms. In addition, working curves are available²¹⁾ from which kinetic parameters may be extracted for varieties of possible reaction mechanisms. The experiment consists of stepping the potential from an initial value (E_i), where no electrode reaction was preceding, to a final value (E_f), where the species of kinetic interest was generated at the electrode surface. The potential was held at E_f for a period of time (τ), after which it was stepped back to E_i and maintained there for the same interval. During this period a portion of the product generated at E_f was converted back to the starting material. In chronocoulometry, the ratio of the two charges, $Q_R = Q_b / Q_f$ (after correction of background contribution as determined in blank experiments) provides a measure of the ratio of any reaction that consumes the product generated at E_f . The experiments are performed by varying the switching duration time (τ) over a suitable range and comparing the results to the theoretical working curves for various mechanisms in an attempt to find a satisfactory match. In solutions of pH 1.68, the chronoamperometric experiment for the reduction of Alizarin Red S was performed on stepping the electrode potential from $E_i = 0.0$ to $E_f = -0.45$ volt for a duration time (τ) and then back to E_i . According to the Cottrell equation,¹⁶⁾ a plot of the cathodic current (i_c) versus $t^{-1/2}$ should therefore be linear with a slope (S) of $nFAC^*(D/\pi)^{1/2}$, where n is the number of electrons transferred, C^* and D are the concentration and diffusion coefficient of the reactant, respectively, and A is the surface area of the electrode for diffusion-controlled processes. Thus, upon plotting i_c as a function of $t^{-1/2}$ for the chronoamperometric results for each value of the switching time used, straight lines are obtained with correlation coefficients of 0.999 for all switching times. These results indicate that, over the entire range of time, the reduction of ARS is diffusion-controlled in nature.¹⁶⁾ From the gradient, the diffusion coefficient of ARS was calculated to be $(1.78 \pm 0.02) \times 10^{-6} \text{ cm}^2 \text{ s}^{-1}$. Such a value of D agrees with that previously reported for 2-quinizarin sulphonic acid.²²⁾

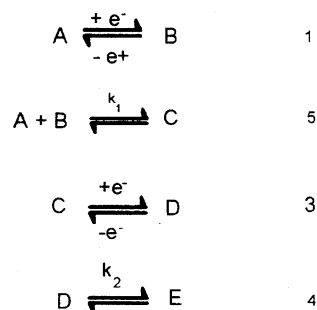
For the chronocoulometric results, it is clear that upon plotting the charge versus $t^{1/2}$, straight lines are obtained with correlation coefficients of 0.999 for all duration times used. This gives additional evidence of the diffusion-controlled nature of the cathodic electrode reaction.¹⁶⁾ Again, the diffusion coefficient was evaluated from the slope of the straight lines obtained, $S = 2nFAC^*(D/\pi)^{1/2}$. The value obtained is $(1.60 \pm 0.03) \times 10^{-6} \text{ cm}^2 \text{ s}^{-1}$, which is in a good agreement with the chronoamperometric value. In order to establish the electrode reaction mechanism and to evaluate its kinetic parameters, the chronocoulometric data obtained were analyzed according to the curve-fitting technique for different electrode mechanisms described by Hanafey et al.²¹⁾

The experimental chronocoulometric curves, the charge ratio (Q_R) as a function of the switching time ($\log \tau$) for a series of switching times (τ), were matched with the theoretical working curves. The appropriate working curves were selected by first finding the curves that give the best fit to the experimental data points. It was found that the experimental results are consistent with the initial hypothesis that the electrochemical reduction of ARS at lower pH's (1.68) proceeds via an ECEC mechanism. The ECEC mechanism comprises three kinetic pathways, as shown in Scheme 1. In the first pathway (a), it is possible that two anion radicals formed in

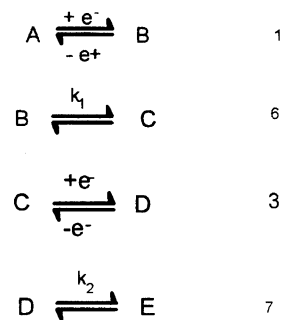
a-ECEC, radical-radical dimerization



b-ECEC, parent-radical dimerization



c-ECEC, first-order

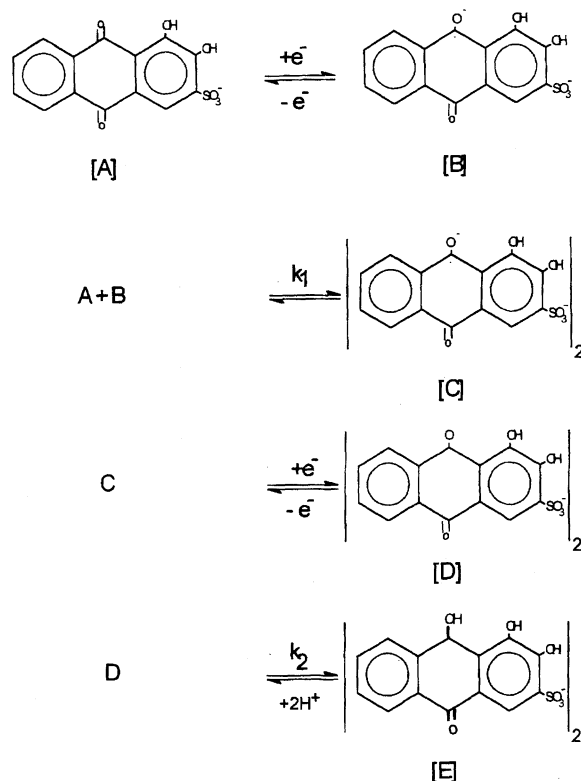


in which A represents alizarin red S in the bulk

Scheme 1.

reaction 1 couple following an ECEC, radical–radical dimerization with $k_2/k_1[A]=0.1$, reaction 2. The second possible pathway (b) is an ECEC, parent–radical dimerization with $k_2/k_1[A]=0.1$, in which reaction 1 is followed by coupling of the parent monomer (A) with the anion radical (B) reaction 5. The third suggested pathway is an ECEC, first-order protonation chemical reaction with a rate-constant ratio (k_2/k_1) of 0.1, in which the chemical reactions (6 and 7) are first order.

As can be judged from Fig. 2, the experimental data satisfactorily accommodate the ECEC, parent–radical dimerization (Scheme 2). A similar mechanism was concluded for the reduction of 2-quinizarin sulphonic acid on a mercury electrode.²²⁾ To calculate the reaction rate constants (k_1 and k_2) the value of the kinetic parameter ($k_1 \tau[A]$) was obtained from the fitted working curves for each corresponding value of the charge ratio (Q_R). From the slope of the $k_1 \tau[A]$ versus τ plot, the rate constant (k_1) value is obtained. The calculated rate constant (k_1) was found to be $(1.52 \pm 0.03) \times 10^3 \text{ M s}^{-1}$ ($1 \text{ M} = 1 \text{ mol dm}^{-3}$). The value of k_2 was estimated from the kinetic term, $k_2/k_1[A]=0.1$, to be $(9.12 \pm 0.05) \times 10^{-2} \text{ s}^{-1}$. Thus, the rate-determining step is the protonation reaction of the dianion dimer. The double potential step chronoamperometry of $6.0 \times 10^{-4} \text{ mol dm}^{-3}$ Alizarin Red S at pH 6.75 is obtained on stepping the potential from $E_i = -0.30$ to $E_f = -0.62 \text{ V}$ and then back to E_i . The dependence of the cathodic current, for each duration time used, on the time, $t^{-1/2}$, was found to be linear with correlation coefficients of



Scheme 2.

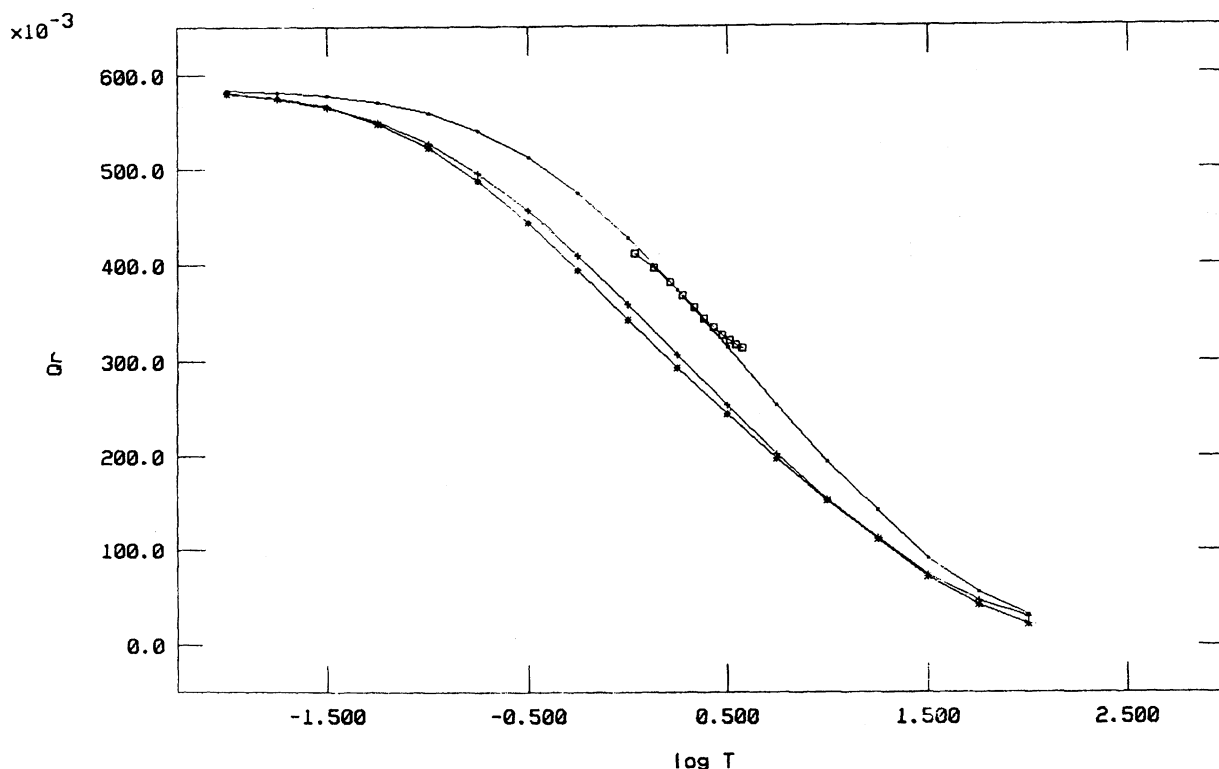


Fig. 2. Best fit of the experimental chronocoulometric data with the theoretical working curves for possible ECEC reduction mechanisms of Alizarin Red S at pH=1.68, **** radical–radical dimer; +++++ parent–radical dimer; □□□ first-order; ◆◆◆ experimental.

0.999. This indicates that ARS is electrochemically reduced at pH 6.75 via a diffusion-controlled process. The diffusion coefficient was determined chronoamperometrically to be $(1.82 \pm 0.03) \times 10^{-6} \text{ cm}^2 \text{ s}^{-1}$. This value is in a good agreement with the above value calculated at lower pH's. On the other hand, an analysis of the chronocoulometric data according to the $Q-t^{1/2}$ relationship, the diffusion-controlled nature of the process was confirmed and the diffusion coefficient for the title compound is $(1.90 \pm 0.02) \times 10^{-6}$ consistent with the above calculated value. The chronocoulometric charge ratios (Q_R) for a series of duration times are fitted with the theoretical working curves of Hanafey.²¹⁾ It can be seen that the experimental data match the working curves for the ECEC mechanisms, c.f. Scheme 1. From this it is also found that the experimental data correctly fit the theoretical working curves for the ECEC, parent-radical dimerization at $k_2/k_1[A]=0.1$. This is indicative of the electrochemical reduction of Alizarin Red S through an ECEC, parent-radical dimerization kinetics. The rate constants (k_1 and k_2) are obtained following the above procedure. They have values of $(3.48 \pm 0.03) \times 10^3 \text{ M s}^{-1}$ and $(20.0 \pm 0.1) \times 10^{-2} \text{ s}^{-1}$, respectively for k_1 and k_2 . This indicates that protonation of the dianion dimer is the rate-determining step. The high values of the rate constants (k_1 and k_2) compared to that at lower pH's can be interpreted as follows. At lower pH's (<5.2) the 1 and 2-OH groups of the subject dye do not dissociate and thus the 1-OH stabilizes the formed anion radical (reaction 1, Scheme 1) by hydrogen bonding. Accordingly, it becomes more difficult to reduce than the neutral radical and dimerizes through C-C dimerization.²³⁾ On the other hand,

at higher pH's (>5.2) the 2-OH group dissociates and becomes hydrogen bonded to the 1-OH. This in turn enhances the dimerization reaction, i.e., the dimerization rate constant (k_1) at such pH's has a high value. This is in accordance with the experimental values obtained, $k_1 = (3.48 \pm 0.02) \times 10^3 \text{ M s}^{-1}$ at pH 6.75 and $k_1 = (1.52 \pm 0.03) \times 10^3 \text{ M s}^{-1}$ at pH 1.68. At $1.44 \times 10^{-4} \text{ mol dm}^{-3}$ Alizarin Red S, the relative peak current of the adsorption pre-wave at -0.245 V and the diffusion wave at -0.322 V increase upon increasing the scan rate (c.f. Fig. 3). At a low scan rate of 50 mV s^{-1} the behavior approaches an uncomplicated diffusion reduction. Upon increasing the scan rate, the adsorption pre-wave appears and increases faster than the diffusion one. At higher scan rates, i.e., $v=800 \text{ mV s}^{-1}$, the adsorption wave becomes dominant. The adsorption current function increases while that for the diffusion one decreases with increasing the scan rate. This supports the conclusion that the pre-wave is due to strong adsorption of the reduction product.²⁴⁾ If the bulk concentration is reduced, the height of the diffusion wave decreases while that of the adsorption one remains constant until at $1.99 \times 10^{-5} \text{ mol dm}^{-3}$ the diffusion peak vanishes and a pair of adsorption peaks are observed there, as shown in Fig. 4. The peak height of the adsorption wave is directly proportional to the scan rate. The proportionality can be represented by the following least-squares relation:

$$\log i_p = -0.146 \pm 0.003 + 1.01 \pm 0.02 \log v, \quad r = 0.998. \quad (5)$$

At a bulk concentration of $5.0 \times 10^{-6} \text{ mol dm}^{-3}$, the title compound gives a pair of symmetric peaks, the anodic peak upon scan reversal is nearly the mirror image of the cathodic

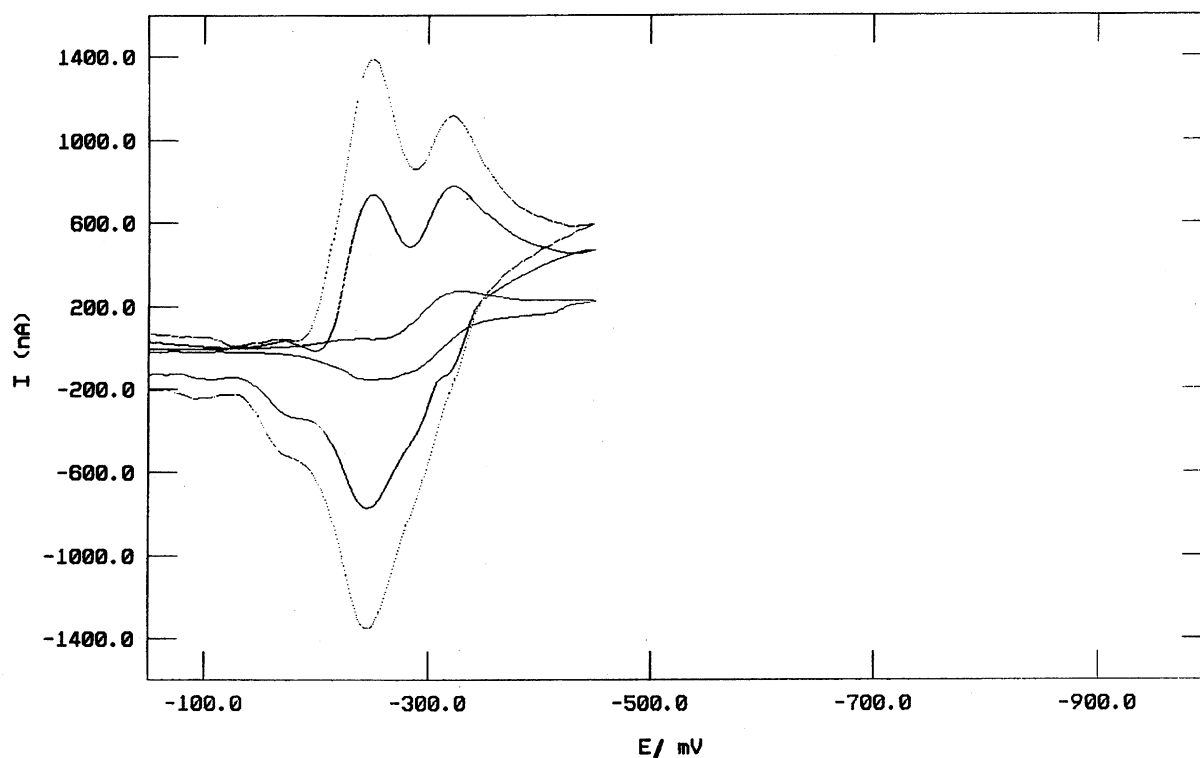


Fig. 3. Cyclic voltammograms of $1.44 \times 10^{-4} \text{ mol dm}^{-3}$ Alizarin Red S at scan rate of 50, 200, 500, and 800 mV s^{-1} at pH=1.68.

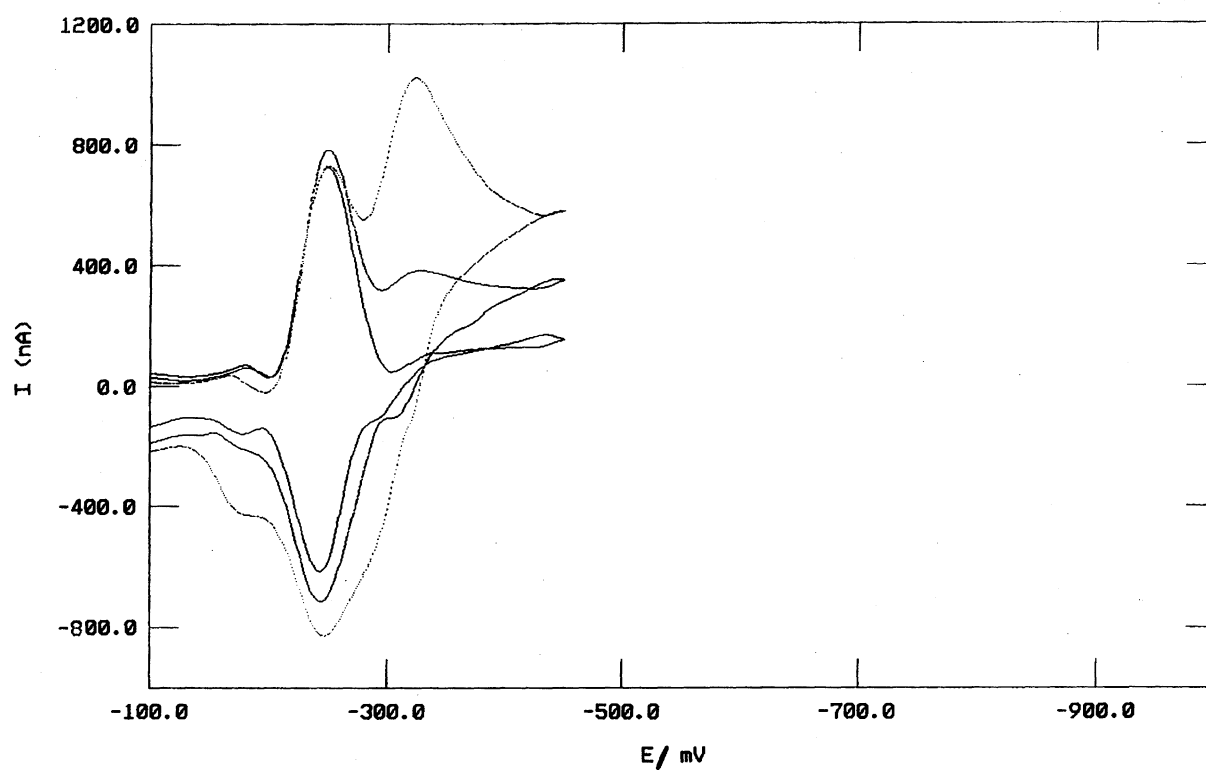


Fig. 4. Cyclic voltammograms of Alizarin Red S at scan rate of 500 mV s⁻¹; pH=1.68 at concentrations of 2.0E-5, 7.0E-5, and 2.1E-4 mol dm⁻³.

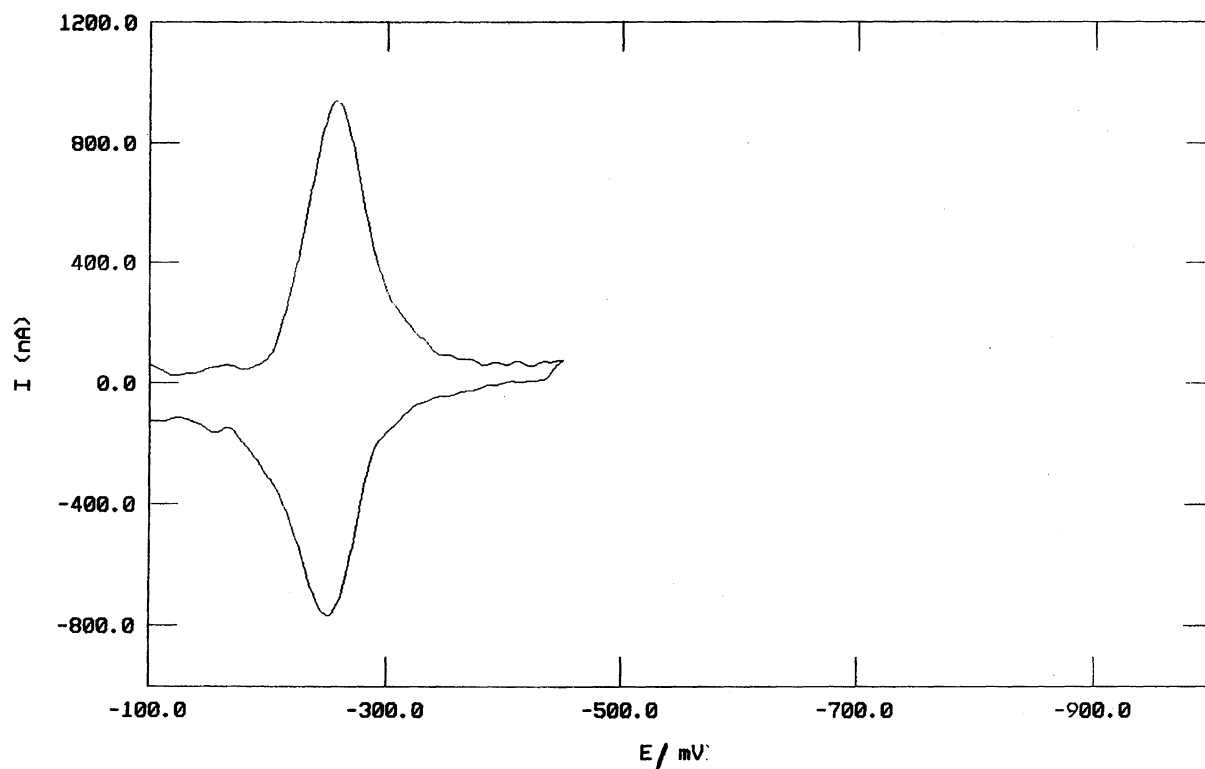


Fig. 5. Cyclic voltammogram of Alizarin Red S at scan rate of 1000 mV s⁻¹; pH=1.68 at concentrations of 5.0E-6 mol dm⁻³.

peak reflected across the potential axis, and their separation ($E_{pa} - E_{pc}$) approaches zero, c.f. Fig. 5. Their symmetries do not vary at high scan rates. These observations are strong evidence for the suggestion that the pre-wave corresponds to the adsorption of a species that undergoes a reversible ideal Nernstian electrochemical reduction in the adsorbed state under the Langmuir conditions.^{16,24,25)}

The number of electrons transferred for the adsorption wave can be determined from the values of the peak width at half-height ($W_{1/2}$) which is $3.53 RT/nF$, i.e., 90.6 mV at 298 K for ideal reversible adsorption peaks.^{24,25)} The observed half-width for the subject quinone is 49.2 ± 0.1 mV for the adsorption reduction peak and 47.6 ± 0.2 mV for the oxidation one. With all other aspects of the peak being nearly ideal, these values suggest that two electrons are involved in the redox couple for the adsorbates, just as for the dissolved species. The amount of adsorbed Alizarin Red S was determined from the area of the cathodic surface peak in the cyclic voltammogram. It is found that the area depends on the substrate bulk concentration, and reaches a limiting value at a higher concentration. They are expressed as the surface excess Γ (mol cm^{-2}) which is estimated using the following equation:¹⁶⁾

$$A(\text{ad}) = nFA\Gamma, \quad (6)$$

where $A(\text{ad})$ is the area of the adsorption peak, A is the electrode surface area and Γ is the surface excess. At a scan rate of 500 mV s^{-1} , where it can be assumed that the adsorption of the product is virtually in equilibrium, the charge obtained at a bulk concentration $\geq 4.6 \times 10^{-5} \text{ mol dm}^{-3}$ is $(9.2-9.6) \times 10^{-8} \text{ C cm}^{-2}$, which is equivalent to a maximum surface excess of $(1.40-1.46) \times 10^{-10} \text{ mol cm}^{-2}$. This corresponds to a surface area occupied by a molecule on the electrode in the adsorbed layer of 1.18 nm^2 . This value is in a good agreement with the surface area per molecule of anthraquinone-2-sulphonate (1.27 nm^2) on a mercury electrode.³⁾ Thus, it is concluded that Alizarin Red S is horizontally oriented on the electrode surface.

The equilibrium surface coverage is a function of the bulk concentration. At a bulk concentration of $4.6 \times 10^{-5} \text{ mol dm}^{-3}$ or higher a limiting coverage is attained, as mentioned above. Upon plotting the surface coverage (Γ_i) as a function of the substrate bulk concentration (c_i), a graph is obtained, as shown in Fig. 6. It is evident that the relationships reminiscent of a Langmuir isotherm, Eq. 6,^{16,25)} is

$$\Gamma_i/(\Gamma_{is} - \Gamma_i) = b_i c_i, \quad (7)$$

where Γ_i is the surface excess of an adsorbed species (i), Γ_{is} is the surface excess at the maximum coverage, b_i is the adsorption coefficient, and c_i is the bulk concentration. It can be linerized in the following form:

$$c_i/\Gamma_i = 1/\Gamma_{is}b_i + c_i/\Gamma_{is}. \quad (8)$$

Upon plotting c_i/Γ_i against c_i , a straight line is predicted. The obtained linear least-squares line can be represented by

$$c_i/\Gamma_i = -(1.3 \pm 0.02)E3 + (8.16 \pm 0.01)E9 c_i, \quad r = 0.998. \quad (9)$$

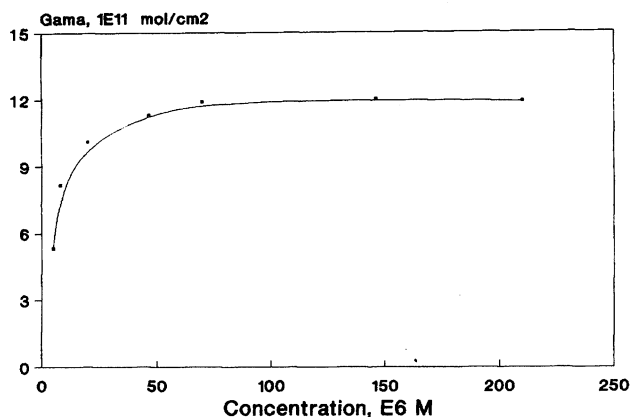


Fig. 6. Relationship between surface excess, Γ_i , and concentration of Alizarin Red S, c_i .

The maximum surface coverage of the adsorbed product (Γ_{is}) is found to be $(1.22 \pm 0.01) \times 10^{-10} \text{ mol cm}^{-2}$, which is slightly lower than the above limiting value. The adsorption coefficient of the adsorbate (b_i) is estimated to be $(5.99 \pm 0.03) \times 10^6 \text{ mol}^{-1}$.

Repeated scans in the potential region of 0.0 to -0.45 V do not show changes in the adsorption or desorption peaks. This reveals that no film of adsorbed material is formed on the electrode surface.

Upon graphing the values of Γ as a function of the bulk concentration, expressed as the negative logarithm, it displays an increase in the surface excess upon increasing the bulk concentration, and then levels off at higher values, c.f. Fig. 7. This indicates that the coverage (and orientation) is essentially an adsorbed monolayer, which remains unchanged as the solute concentration is increased over two orders of magnitude. This is as expected, because the orientation adopted by these species at low concentration already represent the densest packing possible.²⁶⁾ This is in accordance with the early conclusion that anthraquinone disulphonates are not reoriented by the coadsorption of iodine atoms either.²⁷⁾ This resistance to reorientation is probably due to each interaction of the three fused rings with the electrode surface in flat orientation, which would permit only

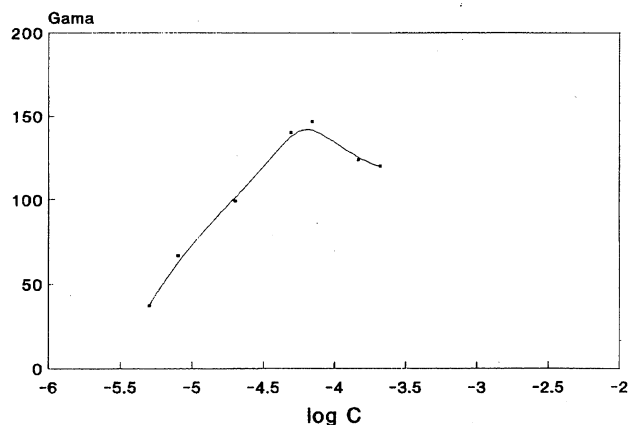


Fig. 7. Relationship between surface excess, Γ_i , and concentration of Alizarin Red S, $-\log c_i$.

a limited interaction.

References

- 1) A. N. Diaaz, *Talanta*, **38**, 571 (1991).
- 2) B. Keita and L. Nodio, *J. Electroanal. Chem.*, **162**, 171 (1984).
- 3) A. Nelson and N. Auffret, *J. Electroanal. Chem.*, **248**, 167 (1988).
- 4) G. A. Qureshi, G. Svehla, and M. A. Leonard, *Analyst*, **104**, 705 (1979).
- 5) G. Feher, R. A. Isaacson, J. D. McElroy, J. E. Ackerson, and M. Y. Okamura, *Biochem. Biophys. Acta*, **368**, 135 (1974).
- 6) A. G. McDermott, V. K. Yachandra, R. D. Guiles, J. T. Cole, S. L. Dexheimer, R. D. Britt, K. Sauer, and M. P. Klein, *Biochemistry*, **27**, 4021 (1988).
- 7) R. A. Morton, "Biochemistry of Quinones," Academic Press, New York (1965).
- 8) F. J. Ruzicka, H. Beinert, K. L. Schepler, W. R. Dunham, and R. L. Sands, *Proc. Natl. Acad. Sci. U.S.A.*, **72**, 2886 (1975).
- 9) N. H. Furman and K. G. Stone, *J. Am. Chem. Soc.*, **70**, 3055 (1948).
- 10) L. A. Wiles, *J. Chem. Soc.*, **1958**, 1358.
- 11) A. D. Broadbent and E. F. Sommermann, *J. Chem. Soc. B*, **1967**, 376.
- 12) G. A. Qureshi, G. Svehla, and M. A. Leonard, *J. Chem. Soc. B*, **1968**, 519.
- 13) G. A. Qureshi, G. Svehla, and M. A. Leonard, *Analyst*, **104**, 1241 (1979).
- 14) H. E. Zitled and T. M. Florence, *Anal. Chem.*, **39**, 320 (1967).
- 15) R. Abdel-Hamid, *J. Chem. Soc., Perkin Trans. 2*, **1996**, 691.
- 16) A. J. Bard and L. R. Faulkner, "Electrochemical Methods, Fundamentals and Applications," John Wiley & Sons, New York (1980).
- 17) R. S. Nicholson, J. M. Wilson, and M. L. Olmsted, *Anal. Chem.*, **38**, 542 (1966); M. L. Olmsted, R. G. Hamilton, and R. S. Nicholson, *J. Electroanal. Chem.*, **41**, 260 (1969).
- 18) E. Laviron, *J. Electroanal. Chem.*, **52**, 355 (1974).
- 19) A. P. Brown and F. C. Anson, *Anal. Chem.*, **49**, 1589 (1977).
- 20) R. S. Nicholson and I. Shain, *Anal. Chem.*, **36**, 706 (1964); **37**, 178 (1965).
- 21) M. K. Hanafey, R. L. Scott, T. H. Ridgway, and C. N. Reilley, *Anal. Chem.*, **50**, 116 (1978).
- 22) F. Capitan, A. Guiraum, and J. L. Vilchez, *Can. J. Chem.*, **59**, 1201 (1981).
- 23) P. J. Elving, *Can. J. Chem.*, **55**, 3392 (1977).
- 24) R. H. Wopschall and I. Shain, *Anal. Chem.*, **39**, 1514 (1967).
- 25) E. Laviron, *Electroanal. Chem.*, **12**, 53 (1982).
- 26) M. P. Soriage and A. T. Hubbard, *J. Am. Chem. Soc.*, **104**, 3937 (1982).
- 27) M. P. Soriage and A. T. Hubbard, *J. Am. Chem. Soc.*, **104**, 2742 (1982).